DOI: https://doi.org/10.4038/sljp.v25i1.8148

INSTITUTE OF PHYSICS – SRI LANKA

Research Article

Spectroscopic analysis of mass-scale prepared GO and rGO from vein graphite through compositional improvement

A M K L Abeykoon[1*], R C L De Silva[1], I R M Kottegoda[1], Yosef Gofer[2], Bruria Shmerling[2]

[1]Materials Technology Section of Industrial Technology Institute, No. 363, Bauddhaloka Mawatha, Colombo 07, Sri Lanka

[2]Department of Chemistry, Bar Ilan University, Ramat-Gan, 5290002, Israel

Abstract

Graphene oxide (GO) and reduced graphene oxide (rGO) were prepared from high pure Sri Lankan vein graphite on a lab-scale as well as on a mass scale following an improved Hummer's method and a thermal method with a goal of investigating the quality of final products. Both oxidation and reduction process in mass scale production process have been subjected to composition and condition change considering factors such as safety, cost-effectiveness, eco-friendliness, user friendliness, and waste disposal management. Raman, XPS, FTIR, XRD, SEM, and TEM spectroscopic analysis were conducted to verify the final products on oxidation of graphite and its successive reduction. Exfoliation of graphite layers into few-layer rGO with large lateral size (D50, *ca.* 45 μm) is visible through TEM and SEM. The XRD, FTIR, and XPS analysis indicated that the graphite was successfully oxidized to GO and reduced back to rGO with fewer oxygen functionalities, equivalent to ca. 7 % wt. The C/O ratio in XPS reflects that the oxygen-containing moieties are twice as rich in GO compared to graphite. XPS and FTIR further revealed epoxide and carboxylic groups being the main oxidized products of GO. Raman spectra further verified the restoration of sp^2 hybridized bonds on the reduction of GO. The rGO prepared at 1000 ºC showed rGO with high conductivity, high surface area, fewest oxygen functions and fewest defects than reported. The combination of spectroscopic analysis carried out in the investigation provided valuable information and knowledge on the chemically produced graphene like rGO on mass scale with good properties compared to similar studies. The study demonstrates directions for further improvement of the synthesis method exploring the ability to use naturally pure vein graphite towards quality graphene on a mass scale.

Keywords: SEM, XRD, TEM, FTIR, XPS, Raman Analysis, rGO, GO, graphene, and Hummers Method

* Corresponding author: lahiru.kulanga@gmail.com

1. INTRODUCTION

Graphene has gained significant interest shortly after its discovery and the award of a Nobel Prize in Physics 2010[1][2]. It has high theoretical surface area of 2630 m^2g, high Young's modulus >1.0 TPa, good thermal conductivity > 5000$Wm^{-1}K^{-1}$, and good electrical conductivity[1][3][4][5]. Its exceptional properties and potential for diverse applications have led acceleration of research and publications in multidisciplinary areas of science. One of the major interests is the mass-scale production of high-quality graphene, using affordable, cost-effective and safe processes to make it competitive in the market. Chemical exfoliation of graphite yields imperfect product. Nevertheless, it is still considered as the most attractive method for producing graphene in terms of scalability and cost-effectiveness[6][7]. Innumerable different methods with their properties have been extensively reviewed for multidisciplinary applications [8][9][10][11]. Among them diverse oxidation methods have been used to prepare GO effectively throughout centuries which are still being considered as promising for a mass scale synthesis of GO. Brodie has introduced oxidation of graphite in 1859[12] which was further developed by Staudenmaier in 1898 [13], Hofmann and Konig in 1937 [14], and Hummers and Offeman in 1958[15]. Recently, Marcano et al. has further improved the Hummers method [16]. The main limitation of these methods are the inherent difficulty of ending up with single-layer graphene, or a pure form of graphene. Oxidation and subsequent reduction of graphite produce rGO, rather than graphene which constitutes neither single-layer nor even few-layer graphene although mechanical, thermal and electrical properties are reasonably similar to graphene. Nevertheless, the product has a huge number of potential applications, in a vast variety of industries, depending on its properties [17][18][19]. Considering the pros and cons of each method, an improved Hummers method was followed here to produce GO on a mass scale in which specific novel aspects were taken to reduce both the cost of raw materials and the burden of the wastewater treatment process. The optimization of the time and energy cost have been done without significant adverse effects on final products. Such a mass scale synthesis and analysis are very limited in the prior art to the best of our knowledge.

After preparing GO, various reduction methods have been followed for preparing rGO from GO. Chemical reduction using reducing agents such as hydrazine is the most common method followed [20][21]. One of the disadvantages of using chemical methods such as hydrazine is the incorporation of heteroatomic impurities into the structure [22]. Moreover, the process cause wastewater treatment complicated. The cost effectiveness, eco-friendliness, user-friendliness, safety and the disposal process are critical factors which must

be considered in the mass scale production. The thermal reduction of GO has attracted as a simple, economical, non-chemical and effective method to produce rGO from past [23][24][25][26]. Efforts to produce rGO by thermal method have also been made in our laboratory recently, which is suitable to produce rGO on mass scale by few minutes [27]. In the present study, the thermal method was further improved to produce graphene like rGO on mass scale. Spectroscopic analysis was conducted to analyze the quality of final products [28]. Since Graphene-based materials has shown interest in a broad spectrum of scientific fields and multiple industries, comprehensive studies on different synthesis methods using graphite is still attracted tremendous attraction. The present work focuses on investigating the quality of GO and rGO produced on a lab-scale and mass-scale from naturally highly pure vein graphite. The quality of rGO can be considered as best if it can be comparable to graphene. Sri Lanka had been the major producer of graphite in the 19th century, producing highly crystalline, pure graphite, with high natural purity [29]. Therefore, with the pure vein graphite from Sri Lanka, it may yield highly value-added products.

2. METHODOLOGY

Naturally pure vein graphite from Ragedara mine of Sri Lanka which has not been subjected to any physical or chemical purification process, was used as the graphite source to prepare GO and rGO. Modified Hummers method [15][30] and a thermal method [31] in literature and method followed in our laboratory were followed to prepare GO and rGO where 1 g of natural graphite was added to 20 ml of concentrated H_2SO_4 at 0 ºC first. Then, 3 g of $KMnO_4$ was added gradually to the mixture while stirring. The mixture was then stirred at room temperature for 30 minutes. 50 ml of water was added slowly to the mixture, which was heated at 98 ºC for 30 min. 150 ml of distilled water was added, followed by 10 ml of 30% H_2O_2 solution. The solids were separated by centrifuge washing with 5% HCl followed by water repeatedly. Different compositions were used for mass scale production of GO from graphite in which case the amount of oxidizing agents used in the lab scale synthesis process were reduced by 20%. The doubled walled reactor connected to a heat and cool circulator was used to produce GO from graphite in this case wherein the oxidation process is completely conducted inside (Figure 1). Even though, the washing process of GO generates considerable volume of wastewater which was managed separately in the mass scale production. Further, we have also followed an optimized thermal method to prepare rGO from GO compared with our previous method [31] in which GO was annealed at 250 ºC for 3 minutes in air and subsequently annealed at 250 ºC , 600 ºC and 1000 ºC in argon for 30

seconds to obtain rGO at 3 different temperatures. During the production of rGO, dried sheets of GO was cut into small pieces before thermal treatment specially in the mass scale production process for safety. In addition, large volume oven was used which sufficiently occupy rGO after formation considering the volume expansion on thermal reduction of GO.

2.1 CHARACTERIZATION

GO and rGO prepared on a small scale and on a mass-scale were subjected to spectroscopic analysis. XRD analysis was conducted using a Bruker D8 Advanced Eco Powder X-ray Diffractometer with Cu K-alpha (λ = 0.154 nm) radiation and a scanning step of 10 (deg/min). The surface morphology of the samples was imaged using a ZEISS EVO scanning electron microscope. TEM was investigated by JEOL 3010 HRTEM operated at an accelerating voltage of 300 kV. Raman analysis was conducted using a Lab RAM Soleil Raman spectroscope at 532 nm. The nominal laser power was 107mW. The powdered samples were measured with a 100x objective, and the others were measured with a 50x ELWD objective. The chemical and structural characteristics of each sample were investigated using a Bruker Tensor 27 FTIR spectrophotometer in the mid-IR spectral range of 600 - 4000 cm^{-1}. X-ray photoelectron spectroscopic (XPS) analysis was carried out using a Thermo Scientific, Nexsa spectrometer (England) equipped with a monochromatic, micro-focused, 72 W Al K-alpha X-ray source (photon energy 1486.6 eV), Beam diameter 400 µm. Survey and high-resolution spectra were acquired at pass energies of 200 eV and 50 eV, respectively. The binding energies of all elements were recalibrated by setting the CC/CH component of the C 1s peak at 284.8 eV. The Brunauer–Emmett–Teller (BET) specific surface area was calculated using a Quantachrome Autosorb IQ analyser with ASiAwin software. Nitrogen adsorption was measured by the volumetric method (196 °C, up to 1 bar). Samples were previously evacuated (P = 0.7 Pa) at 200 °C for 5 h. The conductivity of rGO was measured under different pressure by pressing rGO into cylindrical molds using manual hydraulic press. The pressure was applied to rGO in cylindrical mold from 0.1 to 0.8 MPa. The electrical resistance (R) was measured under the compression using CROPICO DO 5 digital ohm meter. The electrical conductivity (σ) was calculated using the equation, σ = L/AR, where L is the length and 'A' is the cross-sectional area of the cylinder. The conductivity of vein graphite was also measured at 0.8 MPa for comparison. All measurements were repeated three times [32].

3. RESULTS AND DISCUSSION

Hummer's method, and its modified processes [15][16][30][27], have been extensively used to produce GO. Figure 1 depicts the resulting brown colour obtained in the mass scale synthesis of GO as an indication of oxidized GO. Here, we have optimized the raw material composition so that the cost involved in both production as well as wastewater treatment is minimized by considerable volumes. The number of washing cycles, utility of H_2O_2, HCl and water have been simultaneously reduced, dropping the associated material cost, time, and energy significantly. The doubled walled reactor coupled to heating and cooling circulator enclosed all necessary conditions to complete the oxidation reaction safely and successfully. For reduction of GO to rGO also, an optimized time and temperature was followed where the mass scale synthesis of rGO was simply achieved within a few minutes, reducing the time and energy cost significantly.

According to the mechanism, it has been shown that the reduction of GO removes oxygenous groups from the structure resulting rapid evolution of CO and CO_2 gases, creating massive pressure between graphene layers [33][25]. It results explosion causing severe safety issues in the mass scale production process as experienced in this study which is not much prominent in the small scale synthesis using few grams of graphite. It has been reported that a pressure equivalent to *ca.* 40MPa and 130 MPa are generated at 300°C and 1000°C respectively [25]. Therefore, mass scale production of rGO was conducted at low temperature first in argon for few minutes. Due to high volume expansion, it is desired to have sufficient space in the oven to occupy the mass scale produced rGO. Upon thermal treatment, GO puffs like popcorn into a host of tiny black-colour particles, which are easily blown in to the air due to its fluffiness and lightweight. 85g of rGO in a 5L beaker displayed in Figure 1 indicates the lightness of rGO obtained in the present study.

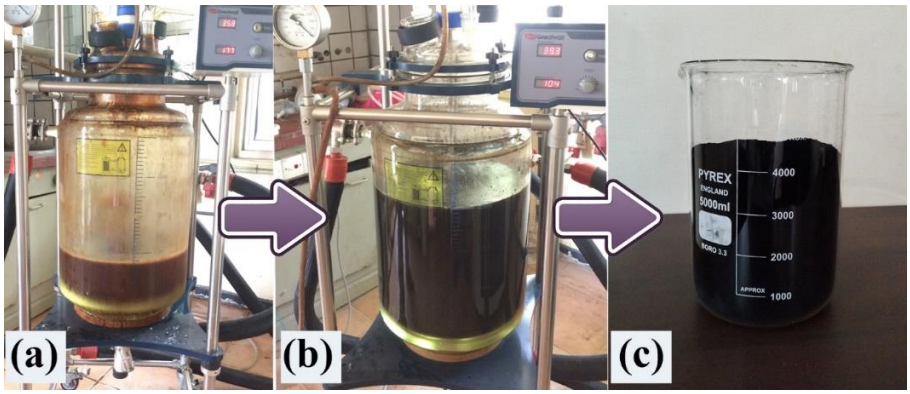

Figure 1: Real images of GO before (a) and after (b) adding water, and thermally reduced rGO (c) in mass scale process.

The resulting rGO of average particle sized *ca.* 45 µm are rolled up naturally and orient freely, with some similarity to saw-dust from wood planer. BET surface area of rGO annealed at 250°C is 465 m^2/g which is higher than many similar studies at that temperature [34]. The bulk conductivity of rGO prepared at 1000°C measured under different applied pressure is shown in the Table 1. An exponential increase of conductivity with increasing pressure is observed wherein a rapid increase from 384.6 to 833.3 S/m is observed with increasing pressure from 0.7 to 0.8 MPa. The conductivity of vein graphite used in this study showed very high conductivity of 3239 S/m at 0.8 MPa pressure which is higher or comparable with reported values and commercial samples [32][35].

Table 1: Bulk conductivity of rGO annealed at 1000 °C under different pressure.

Pressure (MPa)	**Conductivity S/m**
0.1	94.3
0.2	111.1
0.3	125.0
0.4	142.9
0.5	161.3
0.6	208.3
0.7	384.6
0.8	833.3

The rGO obtain at 250°C may contain about 5 or fewer graphene layers compared to the theoretical surface area of graphite, *ca.* 2630 m^2g. Various physical properties of graphite, GO and rGO are shown in the table 2. The rGO produce in this study has very low bulk density which is much better than most of the commercially available rGO, showing its potential for various high-end applications.

Table 2: Physical properties of GO and rGO

	Graphite	**GO**	**rGO**
Colour	Silver gray	Brown	Black
Form	Powder	Sheets	Powder
particle size (D50)	53 µm	variable	45 µm
Bulk density (g/cm^3)	1.02	0.97	0.02
Electrical conductivity (S/m) at 0.8MPa	3239	-	833
Inter layer spacing (Å)	3.325	7.52	3.55

Various oxide functional groups are formed and bound to the graphite structure on oxidation of graphite whereas subsequent reduction technique reduces the oxygen functionalities and produce rGO. Therefore, GO is consisting of both sp^2 and sp^3 hybridized carbon atoms in the structure [36]. However, the reduction of graphite oxide rarely results in pure graphene reestablishing all sp^2 hybridized carbon atoms in the structure. Instead, so called reduced graphene oxide (rGO), consisting of individual graphene particles and multilayer graphene ones, with some remaining oxygen functionalities forms. Hence, it is extremely important to understand the nature of these functional groups and their relation to the oxidation and reduction processes, so that complete reduction of the graphite oxide to pure graphene is realized. The present study used a series of spectroscopic techniques to identify the nature of oxide functions in GO and rGO synthesized in this study.

3.1 XRD and TEM Analysis

XRD spectra of graphite, GO, rGO, and TEM images of rGO prepared on mass scale are shown in Figure 2.

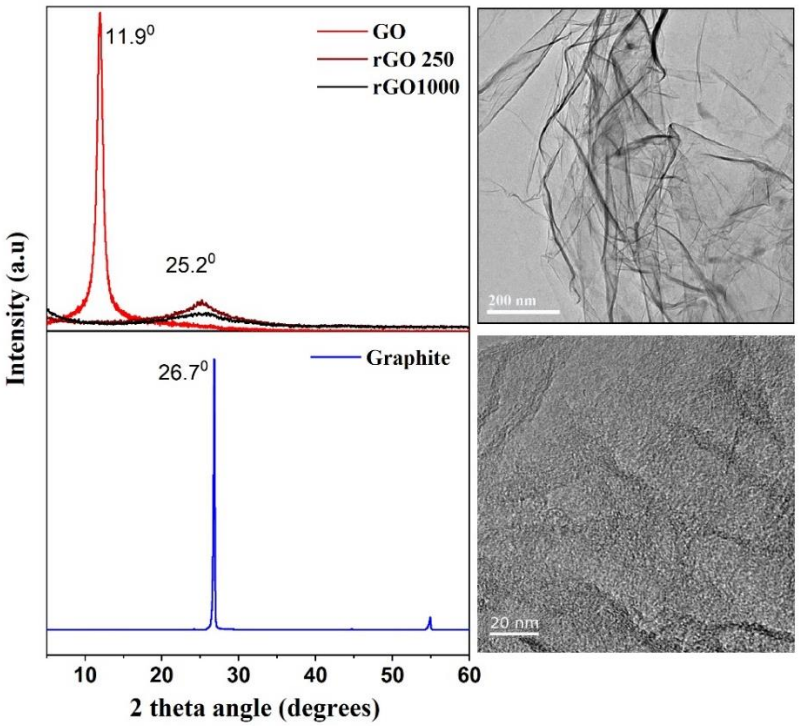

Figure 2: XRD spectra of rGO, GO, graphite and TEM images of rGO 250 ºC

TEM imaging of rGO views as thin corrugated structure of large micro size sheets of rGO which may include few layers of graphene [34]. XRD is a nondestructive technique to identify crystalline phases and determine structural properties such as lattice parameters,

particle size, phase composition, etc. In the present study, the phase change upon oxidation and subsequent reduction of graphite provides useful structural information regarding graphite exfoliation. XRD spectra exhibit respective characteristic 2θ peaks at about ~ 26.7º for graphite, *ca.*11.9º for GO and from~24.8º to 25.2º for rGO synthesized at 250 ºC to 1000 ºC respectively [30][20][37]. The corresponding *d*-values are 3.33 Å, 7.52 Å, and 3.58 to 3.55 Å respectively. The vein graphite used in this study has shown unique properties as shown in Table 2. It is highly conducting and crystalline. The *d*-spacing is unique, 3.325 Å, which is lower than most of the reported value for pristine graphite [28]. In these studies degree of graphitization has been calculated based on Franklin's work in 1951 in which a mean value of 3.354 Å is considered for inter-layer spacing of graphite [38]. The vein graphite used in this study has a lower inter-layer spacing than the above mean value. Therefore, degree of graphitization of vein graphite can be considered as 100% based on these two studies [28] [38].

The 2θ peak at *ca.*11.9º in Figure 2 verifies the entire formation of GO from graphite successfully, while *d*-spacing increases from 3.33 Å to 7.52 Å due to increased layer spacing of GO on oxidation of graphite. The XRD analysis of GO produced on a mass scale showed a similar spectrum except a light change in the main peak which appears at *ca.*11.8º and corresponding *d*-spacing of GO is 7.52 Å which is same as that produced at laboratory scale. The figure is not shown here due to similarity. However, the *d*-spacing value is not that high in small scale and mass scale synthesis process in this study compared to some other publications where Hummer's method with sodium nitrate has been used and showed very high values ranging from 0.9 to 1.0 nm [34]. However, their rGO produced at temperatures ranging from 300°C to 1000°C shows BET surface area ranging from 200 to 350 m^2/g which is lower than even rGO produced at 250°C in this study. A rapid increase in surface area of graphite happens on the conversion of GO to rGO [20].

The thermal conversion of GO to rGO is supported by the new XRD peak corresponding to rGO at 2θ ~24.8º, while the peak corresponding to GO at 11.9º is disappeared. The 2θ angle of rGO is not at the same position as graphite, verifying the phase difference in the presence of oxygeneous groups in rGO. The *d*-spacing has reduced from 7.52 Å to 3.58 Å in forming rGO from GO indicating the restoration of the graphite structure to a great extent. Further decreasing the *d*-spacing to 3.55 Å at 1000 ºC indicates further removal of oxygenous group on further annealing. However, the *d*-value for rGO is still slightly higher than the native graphite (3.33 Å). This is obviously due to the structural changes brought by the oxidation

process [37][39] which are not eliminated entirely on reduction of GO. Hence referring the product in here as rGO rather than graphene is more appropriate. However, the fast synthesis approach seems to be effective in mass production of rGO from GO within few minutes. The rGO was annealed at 1000 ºC for 30 seconds only and enhancement of annealing time or temperature, would further eliminate oxygenous groups from the rGO structure transferring sp^3 hybridized carbon atoms entirely to sp^2 which is among future studies. The shift in 2θ angle, broadness and the low intensity of rGO peak compared with graphite and GO justifies that rGO formed at 250 ºC is few-layer graphene and that at 1000ºC is fewer and containing lesser oxygenous groups [34], comparing to the former studies in our laboratory [30][20]. One of the conclusions drawn at this stage is that under the current experimental condition, the thermal treatment at 1000ºC was even not sufficient in eliminating all the oxygen functionalities in GO while a significant amount is removed which was further verified by FTIR and XPS analysis.

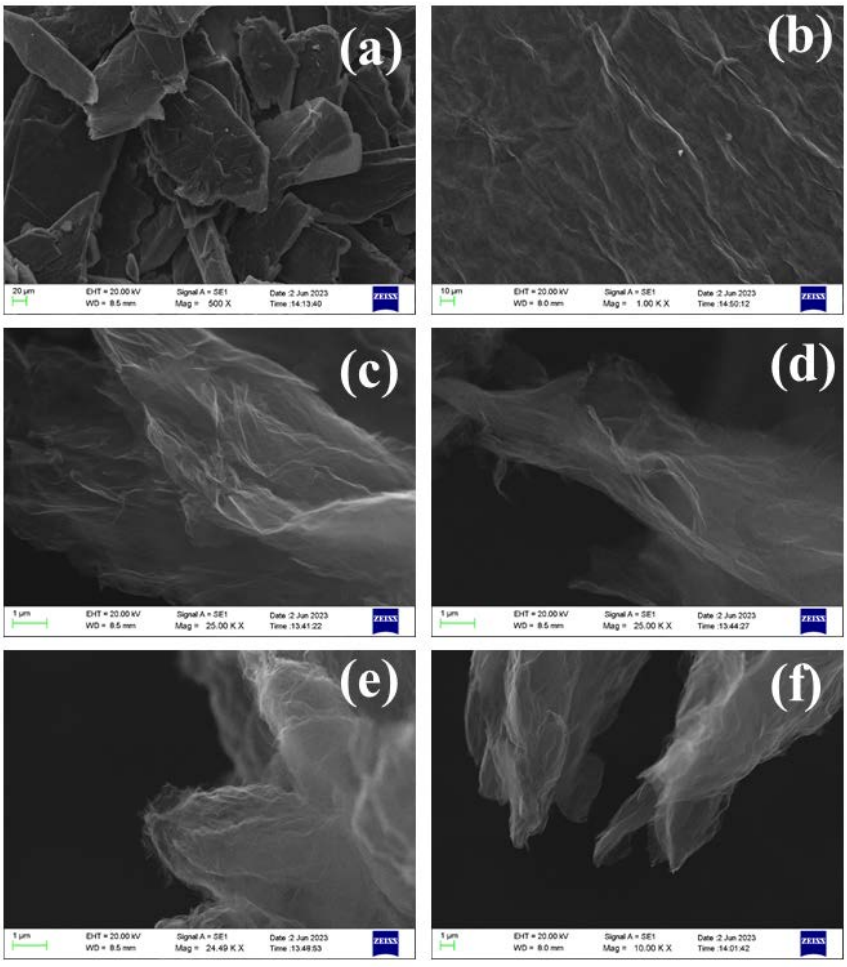

Figure 3: SEM of Graphite (a), GO (b) and rGO prepared at 250ºC in air (c), at 250 ºC (d), at 600 ºC (e) and at 1000 ºC (f) in argon.

Figure 3 shows SEM micrographs of GO, rGO and graphite. Since GO suspension has been dried in a thin layer, GO appears as corrugated thin large size sheets in the SEM micrograph (Figure 3(b)). Both SEM and TEM images of rGO clearly demonstrate that the exfoliation of graphite in to freely oriented thin graphene layers with large lateral size. It is difficult to observe entire particle from SEM analysis to determine the particle size. Moreover, due to the corrugated structure of rGO, it is not possible to measure the lateral size of rGO accurately from SEM. However, the particle size analysis recorded an average particle size of ~ 45μm for GO (not shown here). Transparency observed in SEM image of rGO also witnessed the occurrence of few-layer graphene. While the degree of exfoliation at each temperature is not well understood, the reduction degree of GO can be investigated by observing the remaining oxygen functionalities through FTIR analysis.

3.2 FTIR Analysis

The present study is based on a characterization of similar materials based on graphitic structure. Therefore, uniqueness is very important to distinguish even small structural changes happening in the molecules. The FTIR transmission spectra of graphite, GO and rGO are shown in Figure 4.

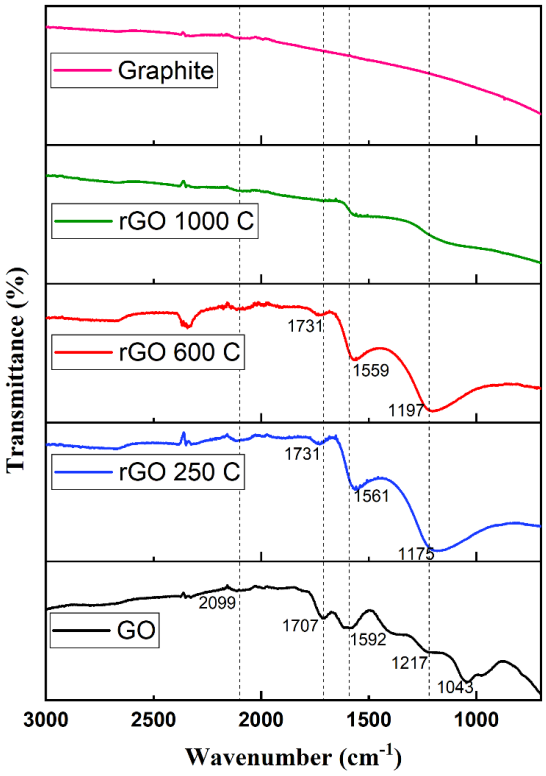

Figure 4: FTIR spectra of Graphite, GO and rGO prepared at 250 ºC, 600 ºC and 1000 ºC

Highly pure graphite was used in the present study, observed to be free from any vibrational peaks whereas reduction to GO produces a series of frequencies corresponding to oxygen-containing functionalities. GO shows characteristics peaks at 1720-1740 cm^{-1} for stretching vibrations of C=O carboxyl groups and C=C from unoxidized sp^2 carbon at 1590-1620 cm^{-1} [15]. Bending and stretching vibrations at 1384 cm^{-1}, 1217 cm^{-1}, and 1043 cm^{-1} for C-OH, C–O–C, C–O groups in the FTIR spectra demonstrate good agreement with previous work [37][39]. After the reduction of GO at 250 ºC, almost all peaks corresponding to oxygen-containing groups such as C-O, C=O, C-O-C, C-OH are reduced to a great extent while complete elimination of C=O and C-OH groups as supported by XPS analysis shown later. The skeleton vibration of un-oxidized graphite is observed at 1561 on restoring sp^2 hybridized C=C bonds on the formation of rGO. Further reduction of C-O groups is observed on further heating at 600 ºC and 1000ºC in argon while rGO prepared at 1000ºC shows elimination of almost all oxygen groups exhibiting similar spectral nature to unoxidized graphite restoring almost all sp^2 domains.

3.3 XPS analysis

Though both FTIR and XPS are widely used for identifying functional groups, XPS is a quantitative surface analysis spectroscopic technique providing information on elemental composition, chemical state, overall electronic structure, and the density of the electronic states of materials by measuring the kinetic energy of electrons emitted from the sample's surface on exposure to soft X-rays [40][41]. By comparing XPS peaks of carbon and oxygen across samples, it is possible to provide considerable qualitative and quantitative information on carbon functionalities, defects, and quality of GO and rGO [42][43]. The relative C/O content in graphite on oxidation and reduction was obtained from the C1s and O1s spectra. The removal of oxygenous groups was also deduced using the XPS high resolution C1s spectra.

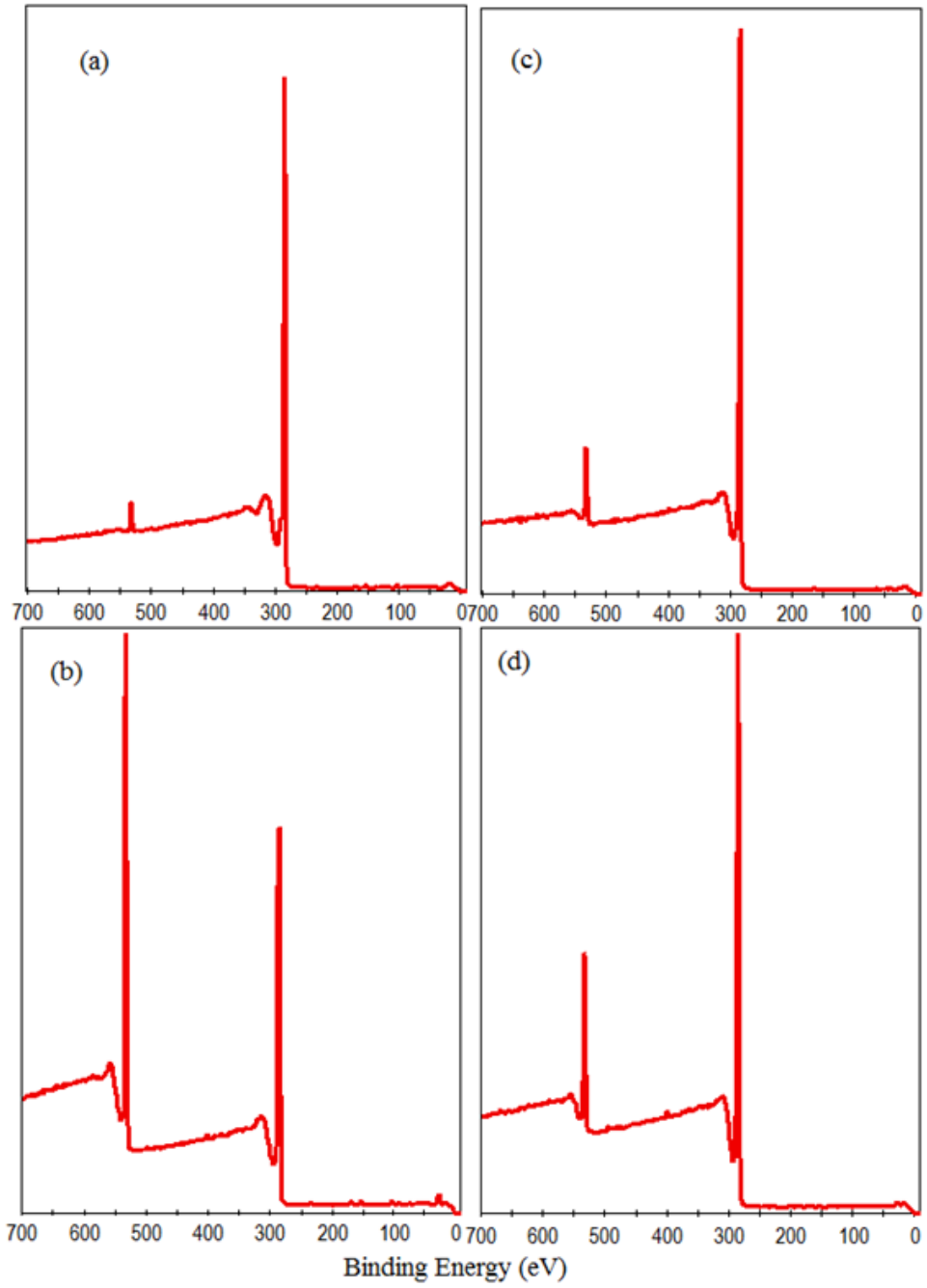

Figure 5: XPS survey spectra of graphite (a) GO (b), rGO 1000ºC (c) and rGO 250ºC (d)

Figure 5 shows the XPS survey spectra of graphite (a), GO (b), rGO 250 ºC (c) and rGO 1000 ºC (d). The general trends in O:C content can be gathered from the respective O1s (at ca. 532eV) and C1s (at ca. 285eV) peaks in the survey spectra. A dramatic increase in oxygen-based groups is observed on oxidation of graphite, and decrease on reduction of GO to rGO. Further decrease is observed for rGO heated at 1000 ºC compared to that at 250 ºC. This is consistent with substantially increased oxygen content and oxygen-based groups as a result of the chemical oxidation of graphite.

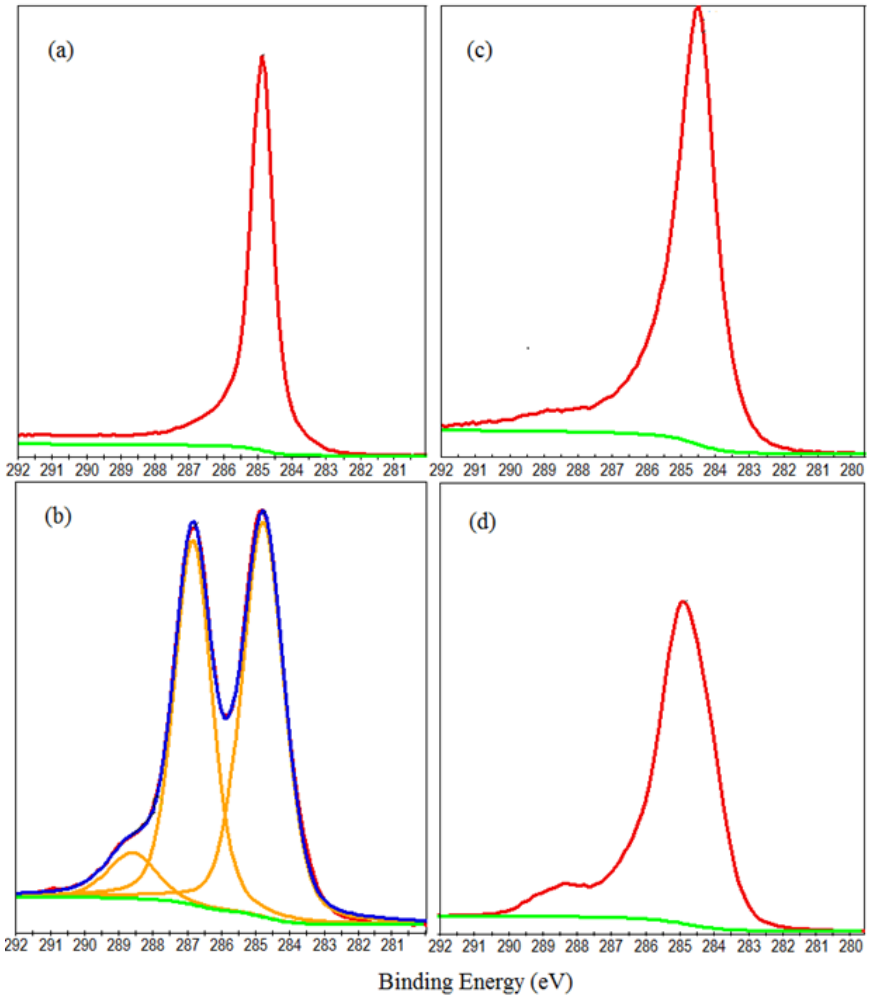

Figure 6: XPS high resolution 1S spectra of graphite (a), GO with peak-fitting (b), rGO 1000ºC (c) and rGO 250ºC (d).

Figure 6 shows the high resolution XPS C1s scan for graphite (a), GO (b), rGO 250 ºC (c) and rGO 1000 ºC (d). The C 1s peak of GO was deconvoluted into three peaks, the minimum number of peaks that gave a sound envelope (Figure 6b) whereas deconvolution of four or more peaks can also be seen depending the prominent peaks based on their results [34]. Here, without post-measurement X-axis shift, the most intense peak at the lowest binding energy (BE) is located at 284.8 eV. This peak can be rationally associated with sp^3 and/sp^2 hybridized carbon atoms, bound to carbon and/or hydrogen only (C=C/C-C). In some studies, C=C and C-C bands were also deconvoluted in to 2 peaks [34]. The strong peak, at 286.8 eV, the 2nd strong peak, can be associated with a wide variety of oxygen-based functional groups (C-O), like ether, epoxide, alcohol, etc. The peak at 288.6 eV can also be related to many functional groups, of higher oxidation states, like aldehydes, ketone, and carboxylates (C=O and O-C=O groups) [44]. Most studies demonstrate deconvolution of

C=O and O-C=O in to 4 main bands. However, the various functional groups observed in this study are in good agreement with FTIR analysis as well. Most of former studies demonstrate deconvolution of the spectra into 4 main components including unoxidized carbon at BE~284.6 eV, carbon in C–O bonds at ~286.0 eV, carbonyl carbon at~288 eV, and the carboxylate carbon (O–C = O), at ~289.0 eV [45][46] [44].

The XPS C1s spectrum of rGO shows a reduction of almost all bands corresponding to oxygen functional groups. However, the spectra were not deconvoluted (Figure 6(c), (d)), as the wide nature of the spectrum and the weak features observed can easily lead to over interpretation. Nevertheless, several core features are clearly visible. The lowest BE peak appears at 284.8 eV, which is also the strongest, can judiciously be associated mainly sp^2 hybridized carbon atoms in C=C bonds. The most of the sp^3 carbon corresponding to oxygen functionalities has been converted to sp^2. Therefore, the spectra appear as a single peak at BE 284.8 eV and tail consisting of smaller peaks in the high BE direction after reduction of GO to rGO at 250°C. The tail to the high BE direction, with the many hindered peaks, can be associated, like before, to a host of oxygen-related functional groups consisting of C-O, C=O and O-C=O. C1s spectra of rGO annealed at 250°C shows (Figure 6(d)) very low intense peak at BE 289 eV corresponding to carboxylate carbon (O–C = O) which has further diminished on further annealing at 1000°C. The results are good agreement with FTIR analysis in which most of the oxide functional groups are removed at high temperature annealing. Other heteroatoms functional groups are not plausible, as no heteroatoms were identified in the XPS analysis, apart from a very small amount, in some cases. Significant oxygen-based functionalities still remain following the thermal treatment at 250 ºC. Despite, rGO heated at 1000 ºC result considerable reduction in O1s peak strength (7% oxygen) resulting graphene like rGO which is in agreement with respective FTIR spectra in Figure 4.

3.4 Raman analysis

Raman spectroscopy has been historically used for analysis of graphitic materials, providing valuable information on degree of exfoliation of graphite into graphene layers, structural defects, and the size of the in-plane sp^2 bonded clusters [46][47][48][36][37]. Accordingly, the occurrence of structural changes during the formation of rGO from graphite was analyzed through the Raman spectroscopy. Figure 7 compares Raman spectra (measured with 532 nm laser) of graphite, GO and rGO. The shape and band positions of Raman spectra obtained for graphite, GO and rGO are common compared with almost all similar prior art.

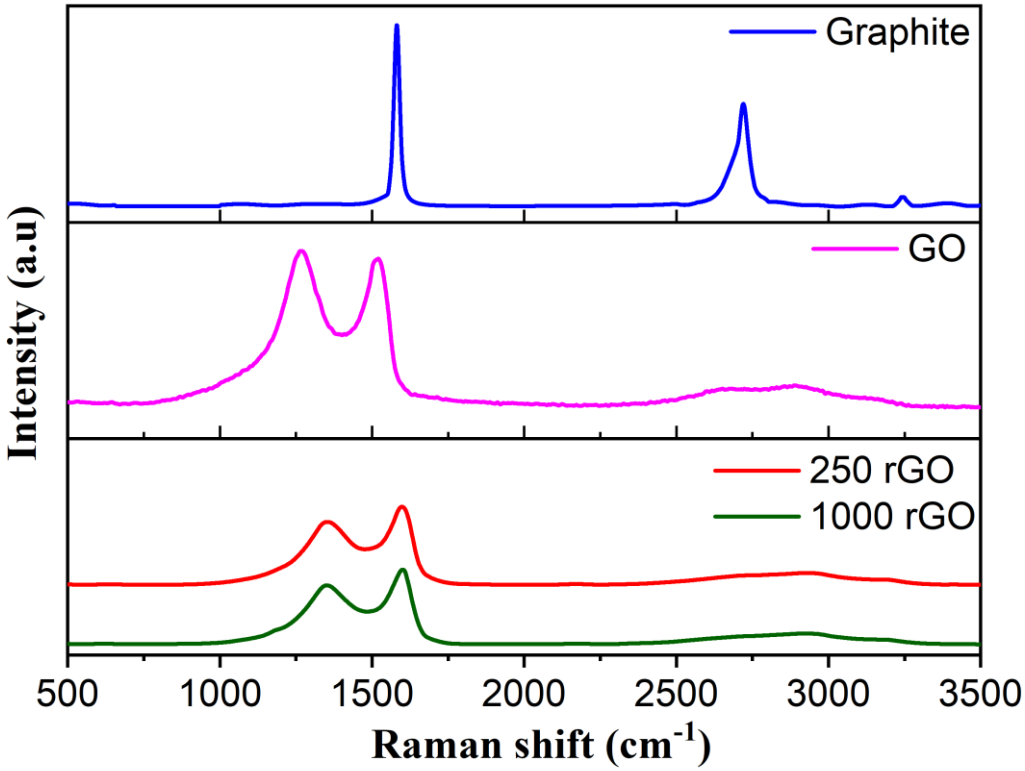

Figure 7: Raman spectra of Graphite, GO, and rGO

The single sharp G band and the absence of D band in Raman spectra of vein graphite indicates that the vein graphite is almost defect free or less. The Raman peaks are not deconvoluted like in some other studies since main features are clearly visible [46]. Weak features observed can easily lead to over interpretation if deconvoluted.

The characteristic feature of carbonaceous materials with conjugated carbon atoms in Raman spectra is the G band which lies at about 1500-1600 cm^{-1}, the D band at 1300-1400 cm^{-1} and the band appears at 2700 cm^{-1} which is known as 2D band [34][46][48][49]. The G band corresponds to bond stretching of all pairs of sp^2 atoms within rings, as well as in chains. D band relates to sp^2 breathing mode of atoms in rings which is not prominent in defect-free graphite [50][51][52][53][54]. First order zone boundary phonons are associated with D band, which present in defected graphitic structures [50][55]. As can be observed, the Raman spectra for both GO and rGO in figure 7, shows a very strong D band with intensity comparable to that of the G band. This reflects conversion of sp^2 hybridized carbon atoms to sp^3. The intense D band, along with a large bandwidth, implies the presence of a significant structural disorder in both GO and rGO compared to graphite. Chemical oxidation of

graphite to obtain GO, and subsequent treatments to form rGO, obviously cause defects in the graphene structure, resulting in highly intense D-band for both GO and rGO. Raman spectra of GO indicate a broad G band on oxidation of graphite due to crystal defects arises from the phonon scattering [48]. G-peak dispersion has been shown to occur from phonon dispersion due to external influence on the structure [48]. Despite the reduction of GO to rGO showed narrowing the G-band and decreasing the D-band compared to the G-band while sharpening the G-band on further heat treatment up to 1000ºC from 250ºC is witnessed whih can be due to the restoration of the graphitic structure on removal of oxygen functionalities. Whereas increased D-band compared to G-band has been observed on reduction of GO to rGO in almost all similar studies [28][34][46] [56].

The G-band of GO at 1604 cm^{-1} has been shifted to 1598-1594 cm^{-1} after reduction to rGO (250ºC-1000ºC), which is consistent with restoration of sp^2 hybridized atoms on oxidation to a great extent. The intensity ratio of the D / G bands, designated as I_D/I_G, has also been used to determine the degree of disorder in graphene arising from edge-planes, charged impurities, ribbed nature and various other factors [48]. The intensity ratio I_D/I_G has decreased from 0.94 to 0.79 on conversion of GO to rGO. I_D/I_G of rGO has further decreased from 0.805 to 0.788 on annealing from 250ºC to1000ºC, indicating an increased sp^2 domain in the structure and partial recovery of the π conjugation in graphene layers on thermal treatment. Obviously, there are more sp^2 domains in rGO compared to GO, even though some sp^3 carbon atoms are still remained. Those sp^3 groups also seems to be reduced considerably on thermal treatment at 1000ºC in which 36% reduction is observed from 250ºC to 1000ºC and attributable to decreasing defects on restoration of sp^2 hybridized carbon in the present study [57][53][54]. Despite, an increased I_D/I_G ratio in rGO has also been observed in some studies and has been explained on different grounds [28][34] [46][56]. Further increasing of I_D/I_G ratio with increasing the temperature has been also noticed in these studies while in the present study decreasing I_D/I_G ratio was observed with further increasing the annealing temperature. They have explained that an intense oxidation and fast thermal exfoliation has caused decreasing the size of the in-plane sp^2, together with increasing the content of edge planes and disorder [52][53][54]. Obviously, rGO with lower defects have been formed in this study compared to these previous works. However, it has been shown that decreasing or increasing the disorder depended on the experimental conditions applied for the synthesis of the materials. We have taken some precautions in the thermal treatment and also used highly pure vein graphite for the preparation of GO and rGO, which presumably results rGO with fewer defects compared to previous studies.

Raman spectra in the range of 500-3500 cm^{-1} in Figure 8 shows different shaped 2D bands for GO and rGO compared to graphite. The 2D band of graphite has shown two components in literature [50][51]. The band at 2900 cm^{-1} has also been referred as a second-order of the D–G bands while band at 2700 cm^{-1} as 2D band [58]. Unlike the D band, which is Raman active only if there are defects in the structure, the 2D band appears even in the absence of any defect. Here we have obtained an additional peak at about 3200 cm^{-1} which has been referred as 2D' which is said to be defect active and is present in graphite with sufficient defects only [59]. Accordingly, defects can have significant impact on 2D band. The intensity ratio of 2900 cm^{-1} band relative to 2700 cm^{-1} band is lower for rGO and lowest for rGO 1000ºC, which indicates decreased defects concentration due to reduce oxygen content in rGO compared to GO[60]. The Raman spectra of both GO and rGO has shown a broad 2D band, which is not comparable to graphite, since its intensity is low for both materials compared with the as-is graphite. According to the shape, shift, and the intensity of the 2D band appears, rGO in the present study can be associated with fewer layers of graphene with some defects compared to prior art as well as the work in our laboratory [31]. AFM analysis would support this attribution in future work.

4. CONCLUSIONS

An improved Hummers method followed by optimized thermal method used in this study found to be viable, user friendly, eco-friendly and effective for the production of graphene like rGO on mass scale from naturally high-pure Sri-Lankan graphite. Under the reported conditions, which are easily scaled-up to industrial quantities yields r-GO of good quality with lower defects than reported. Modifications of the process parameters, like temperatures, time and heating regimes, which are the subject of subsequent studies, may certainly lead to higher reduced r-GO levels and fewer graphene layers. XRD, XPS and Raman analysis provided useful information on defects and the oxidation degree of GO and rGO produced on lab scale and mass scale. The corrugated structure of the rGO could be clearly observed in the SEM and TEM micrographs, showing evidence for the exfoliation of graphite into fewer layers supposed to be five layers in average. BET surface area analysis supported the evidence. On conversion of graphite to GO, the *d*-spacing has changed from 3.33Å to 7.52 Å, as reflected in the corresponding XRD diffractogram which is subsequently reduced back to 3.55 Å on reduction of GO to rGO. XPS analysis reveals presence of two times oxygen w.r.t carbon (O:C) in GO. Although the restoration of all most all sp^2 hybridized bonds has not accomplished, as observed from the Raman analysis, still ca. 92% had been recovered

with decreasing defects. XPS, FTIR and Raman analyses have shown that most of the oxygen-based functionalities inserted during the oxidation to yield GO have been successfully removed on thermal reduction at 1000ºC for 5 minutes and further removal is possible on further increasing the temperature and/or reduction time. It is concluded that although the graphene is not formed through the present method, graphene like rGO consisting lower defects than reported is done on industrial scale with acceptable quality.

Acknowledgement

Financial support from the National Science Foundation, Sri Lanka (Grant No. RG-GAPF-2021-EB-01), National Research council (Grant No. 16/138) and Industrial Technology Institute (Treasury grants) are highly appreciated.

References

[1] A.K. Geim, K.S. Novoselov, The rise of graphene, Nat. Mater. 6 (2007) 183–191. https://doi.org/10.1038/nmat1849.

[2] E. Gerstner, Nobel Prize 2010: Andre Geim & Konstantin Novoselov, Nat. Phys. 6 (2010) 836. https://doi.org/10.1038/nphys1836.

[3] K.I. Bolotin, K.J. Sikes, Z. Jiang, M. Klima, G. Fudenberg, J. Hone, P. Kim, H.L. Stormer, Ultrahigh electron mobility in suspended graphene, Solid State Commun. 146 (2008) 351–355. https://doi.org/https://doi.org/10.1016/j.ssc.2008.02.024.

[4] S. V Morozov, K.S. Novoselov, M.I. Katsnelson, F. Schedin, D.C. Elias, J.A. Jaszczak, A.K. Geim, Giant Intrinsic Carrier Mobilities in Graphene and Its Bilayer, Phys. Rev. Lett. 100 (2008) 16602. https://doi.org/10.1103/PhysRevLett.100.016602.

[5] M.P. Lavin-Lopez, J.L. Valverde, L. Sanchez-Silva, A. Romero, Solvent-Based Exfoliation via Sonication of Graphitic Materials for Graphene Manufacture, Ind. Eng. Chem. Res. 55 (2016) 845–855. https://doi.org/10.1021/acs.iecr.5b03502.

[6] T. Lalire, B. Otazaghine, A. Taguet, C. Longuet, Correlation between multiple chemical modification strategies on graphene or graphite and physical/electrical properties, FlatChem. 33 (2022) 100376. https://doi.org/https://doi.org/10.1016/j.flatc.2022.100376.

[7] A.M.K.L. Abeykoon, R.C.L. De Silva, L.D.C. Nayanajith, I.R.M. Kottegoda, A review on appropriate graphene synthesis methods for diverse applications, Sri Lankan J. Phys. 23 (2022) 125. https://doi.org/10.4038/sljp.v23i2.8116.

[8] F. Farjadian, S. Abbaspour, M.A.A. Sadatlu, S. Mirkiani, A. Ghasemi, M. Hoseini-Ghahfarokhi, N. Mozaffari, M. Karimi, M.R. Hamblin, Recent developments in graphene and graphene oxide: Properties, synthesis, and modifications: A review, ChemistrySelect. 5 (2020) 10200–10219.

[9] T. Sattar, Current review on synthesis, composites and multifunctional properties of graphene, Top. Curr. Chem. 377 (2019) 1–45.

[10] N. Yoshihara, Y. Tahara, M. Noda, Machine learning method for determining chemical vapor deposition conditions for large-area graphene growth, Asia-Pacific J. Chem. Eng. 18

(2023) e2911. https://doi.org/https://doi.org/10.1002/apj.2911.

[11] X. Xu, Q. Wang, X. Zhu, Q. Wu, T. Zheng, H. Yuan, Z. Zhou, The preparation of anti-fouling dual-layer composite membrane with embedding graphene oxide, Asia-Pacific J. Chem. Eng. 18 (2023) e2949. https://doi.org/https://doi.org/10.1002/apj.2949.

[12] B.C. Brodie, XIII. On the atomic weight of graphite, Philos. Trans. R. Soc. London. 149 (1997) 249–259. https://doi.org/10.1098/rstl.1859.0013.

[13] L. Staudenmaier, Verfahren zur darstellung der graphitsäure, Berichte Der Dtsch. Chem. Gesellschaft. 31 (1898) 1481–1487.

[14] U. Hofmann, E. König, Untersuchungen über Graphitoxyd, Zeitschrift Für Anorg. Und Allg. Chemie. 234 (1937) 311–336. https://doi.org/https://doi.org/10.1002/zaac.19372340405.

[15] W.S.J. Hummers, R.E. Offeman, Preparation of Graphitic Oxide, J. Am. Chem. Soc. 80 (1958) 1339. https://doi.org/10.1021/ja01539a017.

[16] D.C. Marcano, D. V Kosynkin, J.M. Berlin, A. Sinitskii, Z. Sun, A. Slesarev, L.B. Alemany, W. Lu, J.M. Tour, Improved Synthesis of Graphene Oxide, ACS Nano. 4 (2010) 4806–4814. https://doi.org/10.1021/nn1006368.

[17] Y.-Z. Wang, X.-Y. Shan, D.-W. Wang, C.-M. Chen, F. Li, H.-M. Cheng, Electrochemical stability of graphene cathode for high-voltage lithium ion capacitors, Asia-Pacific J. Chem. Eng. 11 (2016) 407–414. https://doi.org/https://doi.org/10.1002/apj.2001.

[18] A.D. Sontakke, S. Tiwari, M.K. Purkait, A comprehensive review on graphene oxide-based nanocarriers: Synthesis, functionalization and biomedical applications, FlatChem. 38 (2023) 100484. https://doi.org/https://doi.org/10.1016/j.flatc.2023.100484.

[19] D. Jia, Z. Shen, Y. Lv, Z. Chen, H. Li, Y. Yu, J. Qiu, X. He, In Situ Electrochemical Tuning of MIL-88B(V)@rGO into Amorphous V2O5@rGO as Cathode for High-Performance Aqueous Zinc-Ion Battery, Adv. Funct. Mater. 34 (2024) 2308319. https://doi.org/https://doi.org/10.1002/adfm.202308319.

[20] N.A. Kotov, I. Dékány, J.H. Fendler, Ultrathin graphite oxide–polyelectrolyte composites prepared by self-assembly: Transition between conductive and non-conductive states, Adv. Mater. 8 (1996) 637–641.

[21] S. Stankovich, D.A. Dikin, R.D. Piner, K.A. Kohlhaas, A. Kleinhammes, Y. Jia, Y. Wu, S.T. Nguyen, R.S. Ruoff, Synthesis of graphene-based nanosheets via chemical reduction of exfoliated graphite oxide, Carbon N. Y. 45 (2007) 1558–1565.

[22] W. Gao, The chemistry of graphene oxide, Graphene Oxide Reduct. Recipes, Spectrosc. Appl. (2015) 61–95.

[23] Z.-S. Wu, W. Ren, L. Gao, B. Liu, C. Jiang, H.-M. Cheng, Synthesis of high-quality graphene with a pre-determined number of layers, Carbon N. Y. 47 (2009) 493–499.

[24] H.C. Schniepp, J.-L. Li, M.J. McAllister, H. Sai, M. Herrera-Alonso, D.H. Adamson, R.K. Prud'homme, R. Car, D.A. Saville, I.A. Aksay, Functionalized single graphene sheets derived from splitting graphite oxide, J. Phys. Chem. B. 110 (2006) 8535–8539.

[25] M.J. McAllister, J.-L. Li, D.H. Adamson, H.C. Schniepp, A.A. Abdala, J. Liu, M. Herrera-Alonso, D.L. Milius, R. Car, R.K. Prud'homme, Single sheet functionalized graphene by

oxidation and thermal expansion of graphite, Chem. Mater. 19 (2007) 4396–4404.

[26] Z.-S. Wu, W. Ren, L. Gao, J. Zhao, Z. Chen, B. Liu, D. Tang, B. Yu, C. Jiang, H.-M. Cheng, Synthesis of graphene sheets with high electrical conductivity and good thermal stability by hydrogen arc discharge exfoliation, ACS Nano. 3 (2009) 411–417.

[27] T Chen, Baoqing Zeng, J L Liu, J H Dong, X Q Liu, Z Wu, X Z Yang, Z M Li, High throughput exfoliation of graphene oxide from expanded graphite with assistance of strong oxidant in modified Hummers method, J. Phys. Conf. Ser. 188 (2009) 12051. https://doi.org/10.1088/1742-6596/188/1/012051.

[28] I. Bychko, A. Abakumov, O. Didenko, M. Chen, J. Tang, P. Strizhak, Differences in the structure and functionalities of graphene oxide and reduced graphene oxide obtained from graphite with various degrees of graphitization, J. Phys. Chem. Solids. 164 (2022) 110614.

[29] J.L.R. Touret, J.M. Huizenga, K.V.W. Kehelpannala, F. Piccoli, Vein-type graphite deposits in Sri Lanka: The ultimate fate of granulite fluids, Chem. Geol. 508 (2019) 167–181. https://doi.org/https://doi.org/10.1016/j.chemgeo.2018.03.001.

[30] I.R.M. Kottegoda, N.H. Idris, L. Lu, J.Z. Wang, H.K. Liu, Synthesis and characterization of graphene-nickel oxide nanostructures for fast charge-discharge application, Electrochim. Acta. 56 (2011) 5815–5822. https://doi.org/10.1016/j.electacta.2011.03.143.

[31] I.R.M. Kottegoda, X. Gao, L.D.C. Nayanajith, C.H. Manorathne, J. Wang, J.Z. Wang, H.K. Liu, Y. Gofer, Comparison of Few-layer Graphene Prepared from Natural Graphite through Fast Synthesis Approach, J. Mater. Sci. Technol. 31 (2015) 907–912. https://doi.org/10.1016/j.jmst.2015.07.014.

[32] H. Park, S. Lim, D. Du Nguyen, J.W. Suk, Electrical measurements of thermally reduced graphene oxide powders under pressure, Nanomaterials. 9 (2019) 1387.

[33] S. Pei, H.-M. Cheng, The reduction of graphene oxide, Carbon N. Y. 50 (2012) 3210–3228.

[34] L. Shen, L. Zhang, K. Wang, L. Miao, Q. Lan, K. Jiang, H. Lu, M. Li, Y. Li, B. Shen, W. Zheng, Analysis of oxidation degree of graphite oxide and chemical structure of corresponding reduced graphite oxide by selecting different-sized original graphite, RSC Adv. 8 (2018) 17209–17217. https://doi.org/10.1039/C8RA01486H.

[35] M. Cermak, N. Perez, M. Collins, M. Bahrami, Material properties and structure of natural graphite sheet, Sci. Rep. 10 (2020) 18672.

[36] K.P. Loh, Q. Bao, G. Eda, M. Chhowalla, Graphene oxide as a chemically tunable platform for optical applications, Nat. Chem. 2 (2010) 1015–1024. https://doi.org/10.1038/nchem.907.

[37] T. Szabó, O. Berkesi, I. Dékány, DRIFT study of deuterium-exchanged graphite oxide, Carbon N. Y. 43 (2005) 3186–3189. https://doi.org/https://doi.org/10.1016/j.carbon.2005.07.013.

[38] R.E. Franklin, The structure of graphitic carbons, Acta Crystallogr. 4 (1951) 253–261.

[39] G.I. Titelman, V. Gelman, S. Bron, R.L. Khalfin, Y. Cohen, H. Bianco-Peled, Characteristics and microstructure of aqueous colloidal dispersions of graphite oxide, Carbon N. Y. 43 (2005) 641–649. https://doi.org/https://doi.org/10.1016/j.carbon.2004.10.035.

[40] O.J. Guy, K.-A.D. Walker, Chapter 4 - Graphene Functionalization for Biosensor Applications, in: S.E.B.T.-S.C.B. (Second E. Saddow (Ed.), Elsevier, 2016: pp. 85–141. https://doi.org/https://doi.org/10.1016/B978-0-12-802993-0.00004-6.

[41] D.R. Baer, S. Thevuthasan, Chapter 16 - Characterization of Thin Films and Coatings, in: P.M.B.T.-H. of D.T. for F. and C. (Third E. Martin (Ed.), William Andrew Publishing, Boston, 2010: pp. 749–864. https://doi.org/https://doi.org/10.1016/B978-0-8155-2031-3.00016-8.

[42] L. Torrisi, L. Silipigni, M. Cutroneo, A. Torrisi, Graphene oxide as a radiation sensitive material for XPS dosimetry, Vacuum. 173 (2020) 109175. https://doi.org/https://doi.org/10.1016/j.vacuum.2020.109175.

[43] R. Al-Gaashani, A. Najjar, Y. Zakaria, S. Mansour, M.A. Atieh, XPS and structural studies of high quality graphene oxide and reduced graphene oxide prepared by different chemical oxidation methods, Ceram. Int. 45 (2019) 14439–14448.

[44] C. Xu, X. Shi, A. Ji, L. Shi, C. Zhou, Y. Cui, Fabrication and Characteristics of Reduced Graphene Oxide Produced with Different Green Reductants, PLoS One. 10 (2015) e0144842. https://doi.org/10.1371/journal.pone.0144842.

[45] G. Beamson, High Relution XPS of Organic Polymers. The Scienta ESCA 300 Database, ICIplc. (1992).

[46] T. Anusuya, D.K. Pathak, R. Kumar, V. Kumar, Deconvolution and quantification of defect types from the first order Raman spectra of graphene oxide derivatives, FlatChem. 35 (2022) 100422.

[47] Y. Gogotsi, J.A. Libera, N. Kalashnikov, M. Yoshimura, Graphite polyhedral crystals, Science (80-.). 290 (2000) 317–320.

[48] A.C. Ferrari, Raman spectroscopy of graphene and graphite: Disorder, electron–phonon coupling, doping and nonadiabatic effects, Solid State Commun. 143 (2007) 47–57. https://doi.org/https://doi.org/10.1016/j.ssc.2007.03.052.

[49] R.P. Vidano, D.B. Fischbach, L.J. Willis, T.M. Loehr, Observation of Raman band shifting with excitation wavelength for carbons and graphites, Solid State Commun. 39 (1981) 341–344.

[50] F. Tuinstra, J.L. Koenig, Raman spectrum of graphite, J. Chem. Phys. 53 (1970) 1126–1130.

[51] R.J. Nemanich, S.A. Solin, First-and second-order Raman scattering from finite-size crystals of graphite, Phys. Rev. B. 20 (1979) 392.

[52] K.N. Kudin, B. Ozbas, H.C. Schniepp, R.K. Prud'Homme, I.A. Aksay, R. Car, Raman spectra of graphite oxide and functionalized graphene sheets, Nano Lett. 8 (2008) 36–41.

[53] A.C. Ferrari, J. Robertson, Interpretation of Raman spectra of disordered and amorphous carbon, Phys. Rev. B. 61 (2000) 14095.

[54] M.A. Pimenta, G. Dresselhaus, M.S. Dresselhaus, L.G. Cancado, A. Jorio, R. Saito, Studying disorder in graphite-based systems by Raman spectroscopy, Phys. Chem. Chem. Phys. 9 (2007) 1276–1290.

[55] Y. Zhu, S. Murali, W. Cai, X. Li, J.W. Suk, J.R. Potts, R.S. Ruoff, Graphene and graphene

oxide: synthesis, properties, and applications, Adv. Mater. 22 (2010) 3906–3924.

[56] P. Lian, X. Zhu, S. Liang, Z. Li, W. Yang, H. Wang, Large reversible capacity of high quality graphene sheets as an anode material for lithium-ion batteries, Electrochim. Acta. 55 (2010) 3909–3914.

[57] G. Wang, B. Wang, J. Park, Y. Wang, B. Sun, J. Yao, Highly efficient and large-scale synthesis of graphene by electrolytic exfoliation, Carbon N. Y. 47 (2009) 3242–3246. https://doi.org/https://doi.org/10.1016/j.carbon.2009.07.040.

[58] F.T. Johra, J.-W. Lee, W.-G. Jung, Facile and safe graphene preparation on solution based platform, J. Ind. Eng. Chem. 20 (2014) 2883–2887.

[59] L.G. Cançado, A. Jorio, E.H.M. Ferreira, F. Stavale, C.A. Achete, R.B. Capaz, M.V. de O. Moutinho, A. Lombardo, T.S. Kulmala, A.C. Ferrari, Quantifying defects in graphene via Raman spectroscopy at different excitation energies, Nano Lett. 11 (2011) 3190–3196.

[60] H. Wang, J.T. Robinson, X. Li, H. Dai, Solvothermal reduction of chemically exfoliated graphene sheets, J. Am. Chem. Soc. 131 (2009) 9910–9911.